Int. J. Heat Mass Transfer. Vol. 18, pp. 301–309. Pergamon Press 1975. Printed in Great Britain

AN ANALYSIS OF TEMPERATURE FIELDS IN THE BUBBLE AND ITS LIQUID ENVIRONMENT IN POOL BOILING OF WATER

EJUP N. GANIC* and NAIM H. AFGAN
Boris Kidric Institute, Beograd, Yugoslavia

(*Received* 6 *May* 1974)

Abstract—An experimental analysis of temperature fields in the bubble and its liquid environment is presented. Bubble growth rate is also simultaneously considered. A one-dimensional mathematical model of the temperature field around the bubble is developed and compared with experimental data.

NOMENCLATURE

T, temperature;
T_w, wall temperature;
T_0, temperature of the main body of liquid;
T_{sat}, saturation temperature at system pressure;
R, bubble diameter;
ΔT, $(T_w - T_{sat})$;
T_m, maximum temperature of superheated liquid layer;
g, heat flux at heating surface;
g'', heat flux at bubble interface;
g_L, heat flux into surrounded liquid from superheated liquid layer;
δ, thermal layer (superheated layer of liquid) thickness;
x, spatial coordinate;
$\delta(x)$, Dirac function;
$\theta(x,t)$, $(T - T_{sat})/T_{sat}$;
ΔT_m, $(T_m - T_{sat})$;
λ, thermal conductivity of liquid;
a, thermal diffusivity of liquid;
t, time;
t_0, response time of thermocouple;
k_1, constant defined by equation (12);
k_2, constant defined by equation (13).

INTRODUCTION

PUBLISHING theories considering bubble growth in pool boiling [1–5] are based on the derivation of the bubble growth function $R(t)$ from the solution of the heat energy equation at the liquid–vapor interface. The major difference between these theories is in the ability to predict the temperature gradient at the liquid–vapor interface [6, 9, 10]. The analytical solutions obtained are compared with experimental data for the diameter of bubble which are obtained from high speed photography. The present paper deals with the experimental analysis of bubble growth in pool boiling by following the growth of the bubble by the use of high speed photography and simultaneously measuring the temperature in the bubble and its liquid environment by a fast response thermocouple. The continuous temperature distribution around a single bubble is obtained by changing the position of the thermocouple probe and analyzing a large number of bubbles. A model of temperature fields around a bubble, as a function of spatial coordinate x and time t is developed and compared with experimental data. Special consideration was given to the analysis of the heat flux at liquid–vapor interface. This was compared with the heat flux from the superheated liquid layer to the surrounding liquid.

1. METHODS OF EXPERIMENT PERFORMANCE AND TREATMENT OF EXPERIMENTAL DATA

Experimental apparatus

The experimental apparatus used for this experiment shown in Fig. 1 is specially made for the study of the mechanism of pool boiling [6]. Its heating surface is suitable for filming and visual observation. Due to the

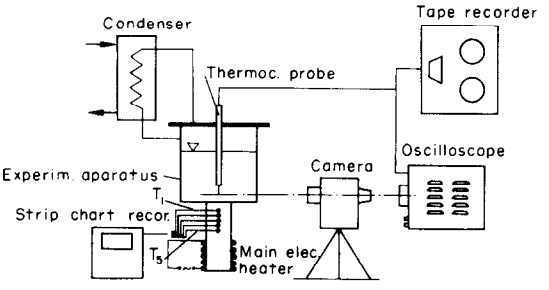

FIG. 1. Schematic diagram of experimental apparatus.

*Now at Massachusetts Institute of Technology, Heat Transfer Lab., Cambridge, Mass. 02139, U.S.A.

suitable construction of the apparatus, heat is transferred to the boiling liquid from the heating surface with only slight loss to the environment. The apparatus is connected with a condenser and a pressure measurement system which permit boiling at the desired conditions for the experiment while keeping the mass constant in the system, e.g. provide a closed system which is essential for the boiling of a multi-component liquid. The total volume of the apparatus which may be viewed by glass windows is 1000 cm^3. A cover is made from stainless steel which has holes in it for inserting tubes for the outflow of vapor and the inflow of condensate, and for the insertion of the secondary heater. The hole in the center of the cover is for the installation of a small tube in which the thermocouple probe is inserted.

The thermocouple, chromel–alumel, which was used for the temperature measurement in the bubble and its liquid environment, was positioned at various distances above the surface test section. It is the most important element of the experimental set-up. It is highly sensitive to small temperature changes in the boiling system and has a relatively short time response to an abrupt temperature change. The method of determining the time constant of the thermocouple is discussed in [7]. For the thermocouple used, the wire diameter is 0·012 mm and the time constant is 0·8 ms for water. The vertical positioning of the tip of the thermocouple is controlled by a micrometer mechanism while the horizontal positioning is controlled by the axial movement of the apparatus cover by special screws.

Due to this arrangement, the tip of the thermocouple probe could be positioned above any point of the test surface section.

The secondary heater which was mentioned previously is U-shaped. It was installed parallel to the heating surface at a distance of 60–40 mm, depending on the level of the liquid in the apparatus.

The heat supplied from this heater is used to completely boil the main body of liquid in the system, depending on the desired experimental conditions.

Method of experimentation

The chamber of the apparatus was first rinsed and then filled with boiled distilled water [8]. After choosing a value for the heat supply, the main and secondary heaters were turned on. The thermocouple probe was positioned above a desired point on the heated surface. The temperature reading from the thermocouple is fed through two amplifiers and then to an oscilloscope. The temperature reading, as a function of time, is now displayed on the oscilloscope for any desired position of the thermocouple probe in the boiling system.

By increasing the power of the secondary heater, the transition from subcooled to saturation boiling was reached. A steady heat supply was controlled by the thermocouples installed in the copper column of the main heater.

In order to study the temperature fields in a bubble and its liquid environment, the growth of a bubble on the heated test section surface was followed by a high speed camera, "Hykam". One lens of the camera was focused on a fixed part of the surface test section while the second lens was focused on the screen of the oscilloscope where the temperature reading was displayed.

Experimental data for analysis are obtained by analyzing the film on which is shown the bubble growth with the corresponding temperature reading in the bubble and its liquid environment during its growth. Real bubble diameter dimensions are found by using as a reference, the known diameter of the thermocouple probe shown in the film and then simply measuring the diameter of the bubble. In the same manner, the determination of the temperature readings is achieved by initially filming a known temperature value and using this as a reference. Filming was carried out at the rate of 4000–6000 frames/s.

Along the border of the film, markings were applied at time intervals of 10^{-3} s. From this information, the real time basis for the film was easily computed. In this way, the complete data for the construction of the experimental curves $R = R(t)$ and $T = T(x_0, t)$ are provided on each film strip.

2. EXPERIMENTAL RESULTS AND DISCUSSION

Shown in Table 1 are the values of the heat flux at the heating surface (for which most of the experimental work was done), the temperature of the heating surface, and the maximum superheat of the liquid (the maximum measured value of temperature between the liquid and vapor in the system).

Table 1

q (W/cm^2)	8·65	17·5	27·7
T_w (°C)	113·9	121·83	125·15
ΔT (°C)	13·9	21·83	25·15

Experimental bubble growth curves and the temperature field changes as the bubble steadily approaches, touches, and finally pierces the thermocouple probe are shown in Fig. 2. The difference in shape of this curve is found for the different position of the thermocouple probe above the test surface.

These curves are obtained by positioning the tip of the thermocouple probe above a single center of nucleation while maintaining a relatively low heat flux at the heating surface ($q = 8{\cdot}65$ W/cm^2) so that the bubble-waiting period will be sufficiently long. On

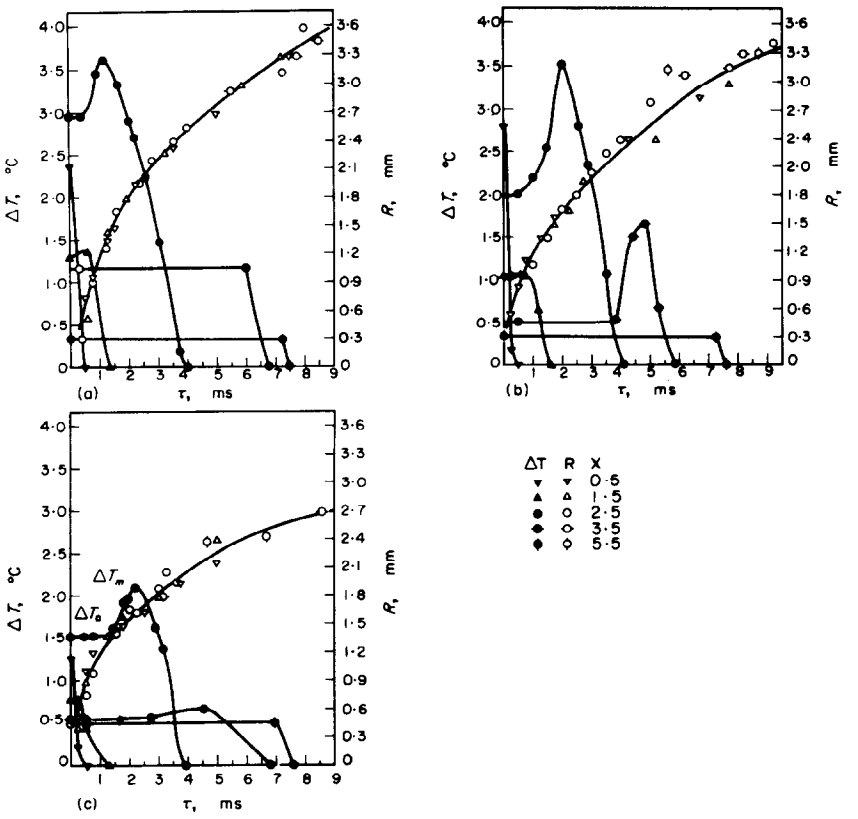

FIG. 2. Change of temperature profile around the bubble during bubble growth (three different bubbles).

ΔT	R	X
▼	▽	0·5
▲	△	1·5
●	○	2·5
●	○	3·5
●	○	5·5

$q = 8{\cdot}65 \times 10^4\ \mathrm{W/m^2}$; $\Delta T = T - T_{\mathrm{sat}}$; $\Delta T_m = T_m - T_{\mathrm{sat}}$; $\Delta T_0 = T_0 - T_{\mathrm{sat}}$; $X(mm)$—distance from heating surface to tip of thermocouple probe.

Fig. 2* one can see that before a bubble approaches the thermocouple, the temperature that is being recorded is that of the main body of liquid, T_0.

As the bubble approaches the thermocouple, the thermocouple first comes into contact with the superheated layer of liquid around the bubble which is shown on the curve by the temperature jump to $T_{\max}$. As the thermocouple probe pierces the bubble, the temperature suddenly drops to the saturation temperature, T_{sat}. It should be noted that the velocity of the superheated liquid layer around the bubble is the same as the bubble growth velocity.

By eliminating the independent variable t from the experimental curves $R = R(t)$ and $T = T(x_0, t)$ we obtain the experimental curves $T = T(R)$ (Fig. 3) which show the change of the temperature field around the bubble as a function of the bubble diameter.

It is clear that due to the temperature difference $T_m - T_0$ (where T_m is the maximum temperature in the superheated layer) that the superheated layer is cooled down by the surrounding liquid. Hence, the heat flux into the surrounding liquid from the superheated layer which is transferred by conduction is:

$$q_L = \lambda \frac{(T_m - T_0)}{\delta_1}. \tag{1}$$

The temperature difference $(T_m - T_{\mathrm{sat}})$ is the driving force of the evaporation process. Therefore, the heat flux supplied to the liquid–vapor interface is:

$$q'' = \lambda \frac{(T_m - T_{\mathrm{sat}})}{\delta_2}. \tag{2}$$

*See especially Fig. 2(c), $x = 2{\cdot}5$ mm.

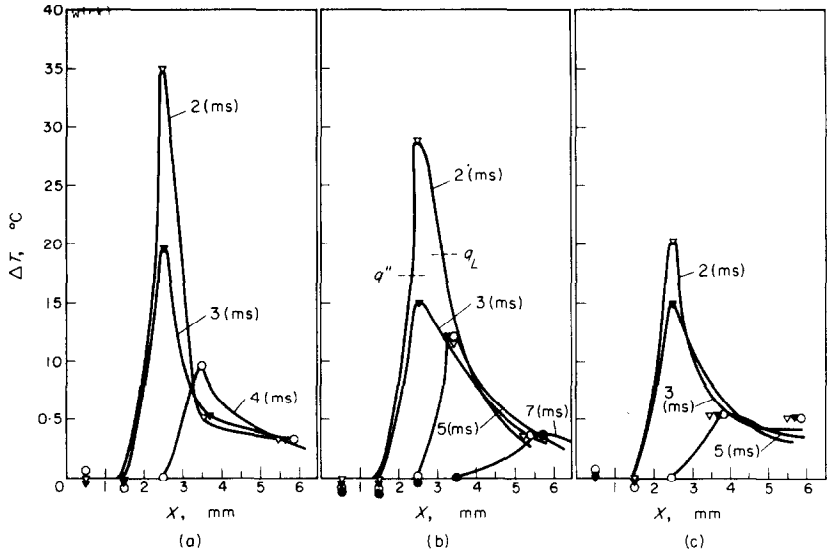

FIG. 3. Temperature profiles around the bubble at several time intervals during growth.

The ratio of these two fluxes is:

$$\frac{q_L}{q''} = \frac{(T_m - T_0)/\delta_1}{(T_m - T_{sat})/\delta_2}. \quad (3)$$

This ratio, approaches zero as x increases (e.g. as the distance between the tip of the thermocouple probe and the test surface increases). This means that the temperature difference between the superheated layer and the main body of liquid decreases as the above distance increases, and that the driving force for the evaporation of the liquid will approach $T_0 - T_{sat}$ (e.g. approach the temperature difference between the main body of liquid and the saturation temperature).

It seems like the same thing happens for the experimental curves obtained at the distances of 0·5 mm and 1·5 mm from the heating surface. In order to explain this the dynamic characteristics of the thermocouple were carefully analyzed. The time response of the thermocouple is 0·8 ms for water. It can be seen from Fig. 2 that the bubble growth rate is very high at the beginning of bubble growth. This means that the velocity of the superheated liquid layer is also very high at the beginning of bubble growth and is in fact equal to the velocity of the bubble growth.

Due to the high velocity of the superheated layer at the beginning of bubble growth (especially for a small distance from the heating surface) or due to the very short time contact of the thermocouple probe with the superheated layer, which is less than the time response of the thermocouple t_0 (Table 2), the thermocouple is not able to show the real value of the temperature of the superheated layer. It is actually showing the temperature of the main body of liquid.

In effect, the thermocouple has a limited frequency range. This explains why the superheated layer around the bubble did not register (no peak on the temperature curve) as the bubble approached the thermocouple probe at the distances of 0·5 mm and 1·5 mm from the heating surface.

The following facts are noted from observing the curves of Figs. 2 and 3:

Table 2

g (W/cm^2)	x (mm)	v (mm/ms)	t_0 (ms)	δ_T (mm)	δ_e (mm)	Δt_t (ms)	Δt_e (ms)
8·65	0·5	2·00	0·8	0·05	0·32	0·025	0·16
8·65	1·5	0·85	0·8	0·05	0·60	0·059	0·70
8·65	3·0	0·30	0·8	0·05	1·00	0·116	3·33

v, velocity of the superheated layer (experimental value);
t_0, time response of the thermocouple;
δ_t, thickness of the superheated layer [$\delta = (\pi a t_w)^{1/2}$];
Δt_t, calculated value for the time interval during which the thermocouple probe is in the superheated layer;
Δt_e, experimental value for the time interval during which the thermocouple probe is in the superheated layer;
t_w, bubble waiting time period [8];
δ_e, experimental values for the thickness of the superheated layers.

There is a superheated layer of liquid around the bubble.

The superheated layer cools down with time, losing heat because of the following:

(a) The evaporation at the liquid–vapor interface.
(b) The heating of the surrounding liquid body.

The maximum temperature in the superheated layer decreases very rapidly at the beginning of bubble growth.

The rate of evaporation on the liquid–vapor interface is determined by the temperature difference $\Delta T = T_m - T_{sat}$.

The actual film which records the bubble growth with the corresponding temperature change around the bubble is shown in Fig. 4. The temperature reading (1), the heating surface (2), and the tip of the thermocouple probe (3) are shown on the film. This qualitative picture shows the complete history of analysis with which this paper deals.

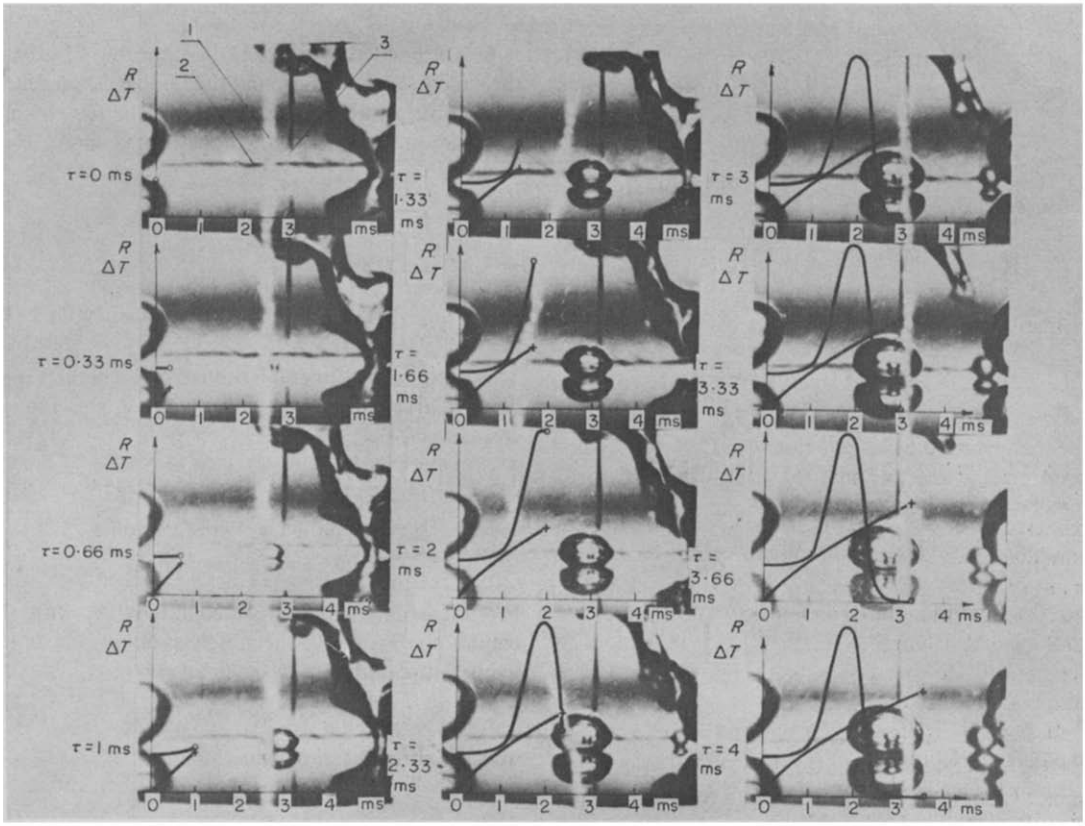

FIG. 4. Analysis of bubble growth.

3. THEORETICAL ANALYSIS

To obtain a function for the change of the temperature profile in the superheated liquid layer around the bubble, one should begin by noting the following. From Fig. 5, it is observed that the thin layer of liquid on the heating surface is first heated up to the temperature T_m. As a bubble grows this superheated liquid layer surrounds the bubble and is pushed away from the surface by the bubble. When the bubble finally leaves the surface it takes with it the superheated liquid layer surrounding the bubble, Figs. 5(b)–(c). The bubble continues to grow by the transfer of heat from the superheated layer which surrounds it.

Before the appearance of a bubble ($t < 0$) at the position $x = 0$ [Fig. 5(a)], the temperature is T_m, which is the temperature of the superheated layer. Due to the very small thickness of the superheated layer, for all practical purposes the temperature at $x = \delta$ can be considered to be T_m. For $x > \delta$ the temperature decreases to that of the main body of liquid T_0, which for this case is equal to or higher than the saturation temperature, T_{sat}.

The temperature distribution at the instant $t = 0$ as a function of spatial coordinate x (distance from the heating surface) is shown on Fig. 6(a); while the temperature distribution as a function of time at the point $x = 0$ is shown on Fig. 6(b). With the appearance of a bubble [Fig. 5(b)] at the position $x = 0$, the vapor

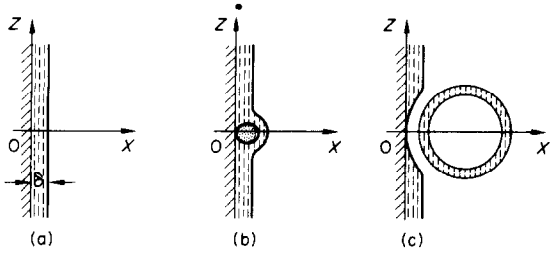

FIG. 5. Simplified model of bubble growth.

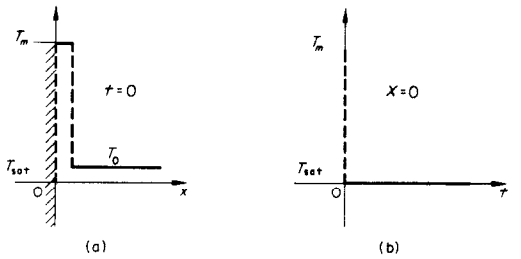

FIG. 6. Simplified model.

phase appears at the temperature T_{sat}. Assuming that the temperature is a function only of the spatial coordinate x and the time t, the previous discussion may be written mathematically as:

$$T(x=0,\ t<0)=T_m \tag{4}$$

$$T(x<\delta,\ t<0)=T_m \tag{5}$$

$$T(x>\delta,\ t>0)=T_0 \tag{6}$$

$$T(x=0,\ t>0)=T_{sat} \tag{7}$$

$$T(x=\infty,\ t>0)=T_0. \tag{8}$$

Heat from the superheated layer is transferred to the liquid–vapor interface ($T_m > T_{sat}$) and to the surrounding liquid ($T_m > T_0$).

The mathematical analysis is based on the use of the following equation with the boundary and initial conditions stated in equations (4)–(8).

$$\frac{\partial T}{\partial t}=a\frac{\partial^2 T}{\partial x^2}. \tag{9}$$

The Dirac function (8) is used to approximate the temperature distribution at $t=0$.

Introducing a new variable, defined as:

$$\theta(x,t)=\frac{T-T_{sat}}{T_{sat}}$$

and by using the Dirac function:

$$\theta(x=0,t)=k_1\delta(t) \tag{10}$$

$$\theta(x,t=0)=k_2\delta(x) \tag{11}$$

where k_1 and k_2 are defined by the relations:

$$k_1=\int_{-\infty}^{\infty}\theta(x=0,t)\,dt \tag{12}$$

$$k_2=\int_{-\infty}^{\infty}\theta(x,t=0)\,dx. \tag{13}$$

from applying the Laplace Transform, the solution of equation (9) is obtained in the form:

$$T(x,t)-T_{sat}=\frac{k_2 T_{sat} x}{2(a\pi t^3)^{\frac{1}{2}}}\exp\left(\frac{-x^2}{4at}\right). \tag{14}$$

In order to take into consideration the velocity of the superheated layer around the bubble as a result of the bubble growth, the final form of the temperature distribution function in the superheated liquid layer around the bubble is:

$$T(x,t)-T_{sat}=\frac{k_2 T_{sat}[x-\beta(at)^{\frac{1}{2}}]}{2(a\pi t^3)^{\frac{1}{2}}}\times\exp\left[\frac{-[x-\beta(at^2)^{\frac{1}{2}}]}{4at}\right]H[x-\beta(at)^{\frac{1}{2}}]. \tag{15}$$

This equation describes the cooling down of the superheated layer during bubble growth on the heating surface.

β, constant of bubble growth
$\beta(at)^{\frac{1}{2}}$, bubble growth function
H, Heaviside function.

From the differentiation of equation (15) with the condition $\partial T/\partial x=0$, the abscissa of the maximum temperature in the superheated layer is:

$$x_m=(2at)^{\frac{1}{2}}+\beta(at)^{\frac{1}{2}} \tag{16}$$

with the corresponding value:

$$\Delta T_m=\frac{k_2 T_{sat}}{(2\pi e)^{\frac{1}{2}}}\frac{1}{t}. \tag{17}$$

A comparison of equation (17) with the experimental data is shown in Fig. 7. The region of the thermocouple inaccuracy which was discussed previously is shown on the diagram.

If the difference between the abscissas corresponding to the maximum ordinates of the temperature experimental curves is divided by the corresponding time intervals, then the result obtained is the velocity of propagation of the maximum temperature in the superheated layer during bubble growth $[V_{TT}+(dR/dt)]$, which is the sum of two velocities: the velocity of the bubble growth dR/dt and the velocity of propagation of the maximum temperature in the superheated layer relative to the bubble interface V_{TT}. The difference between the velocity of propagation of the maximum

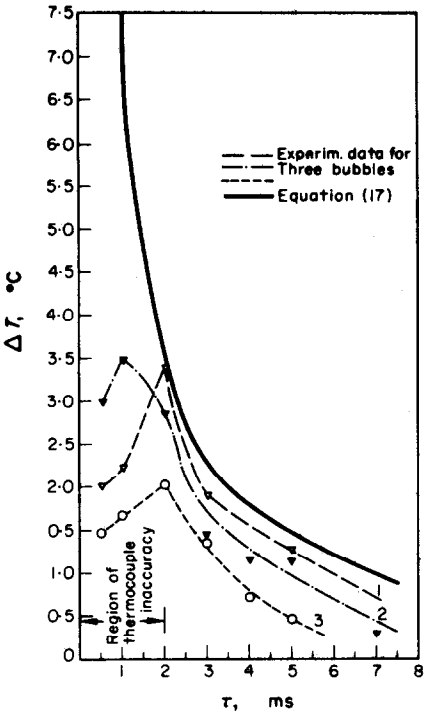

FIG. 7. Comparison of model with data for the maximum temperature in the superheated layer vs time.

temperature and the velocity of the bubble growth is expressed as:

$$V_{TT_s} = k\left(V_{TT} + \frac{dR}{dt}\right) - \frac{dR}{dt} \tag{18}$$

where the constant k corrects for the order of magnitude error present in the temperature derived data and in the diameter measured data.

The theoretical value of the propagation velocity of the maximum temperature in the superheated layer, relative to the bubble interface, which is derived from equation (14) is compared with the experimental values on Fig. 8. Also shown on this diagram is the curve derived from equation (4) [3].

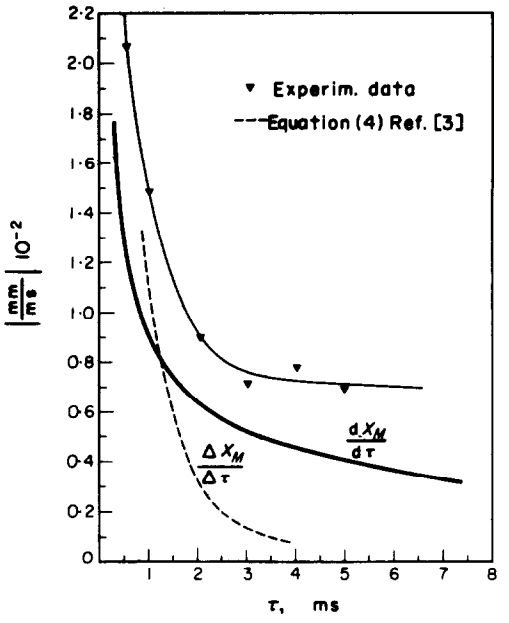

FIG. 8. Velocity of propagation of maximum temperature in superheated layer relative to bubble interface.

From the differentiation of equation (17), we obtain the velocity of the maximum temperature change in the superheated layer

$$\left|\frac{\partial T_m}{\partial t}\right| = \frac{k_2 T_{sat}}{(2\pi e)^{\frac{1}{2}}} \frac{1}{t^2}. \tag{19}$$

This is compared with the experimental data for three bubbles on Fig. 9.

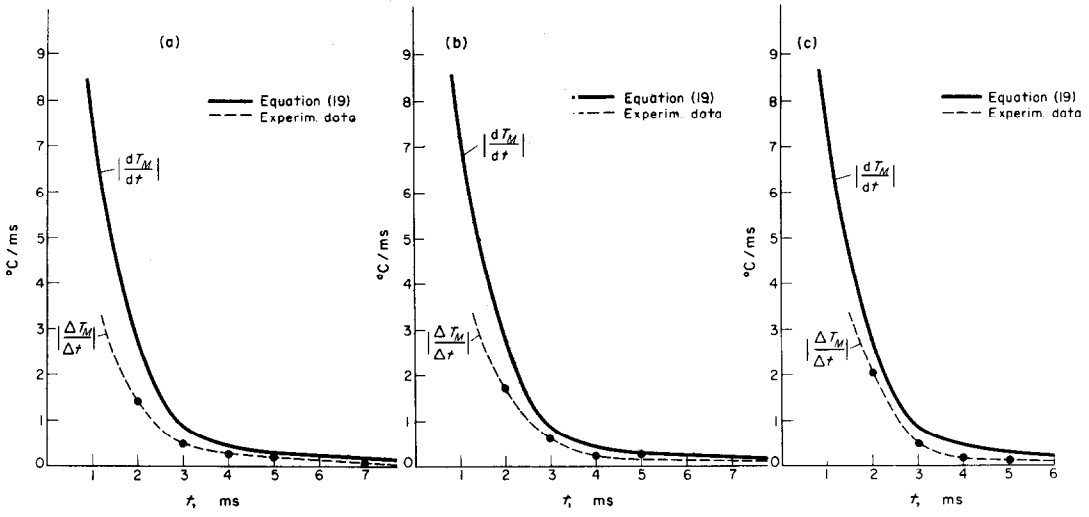

FIG. 9. Comparison of experimental data with model for the transient cooling of the superheated layer.

From a numerical treatment of the data on Figs. 2 and 3, we obtain the value for the temperature gradient on the liquid–vapor interface (bubble interface).

$$\left|\frac{\Delta T}{\Delta x}\right|_{x=R}$$

The heat flux on the interface is:

$$q'' = \lambda \left.\frac{\partial T}{\partial x}\right|_{x=R}$$

and its change with time is shown on Fig. 10. The flux from the superheated layer into the surrounding liquid is defined as:

$$q_L = \lambda \left.\frac{\partial T}{\partial x}\right|_{x=R+\delta}$$

and its change with the time is shown on Fig. 11. The ratio of these two fluxes vs time (during bubble growth is shown on Fig. 12).

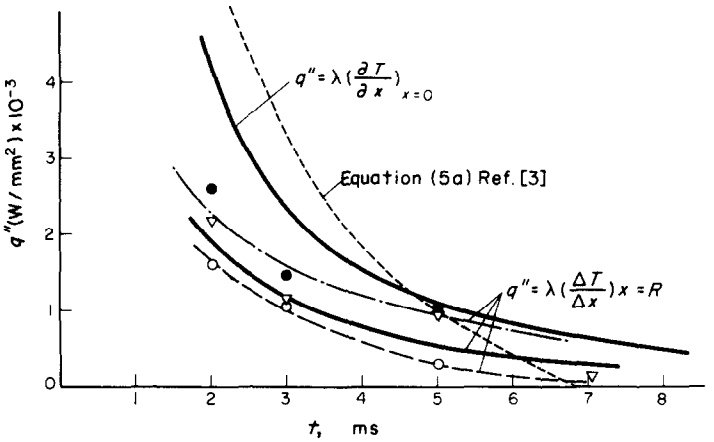

FIG. 10. Heat flux at the bubble interface during bubble growth.

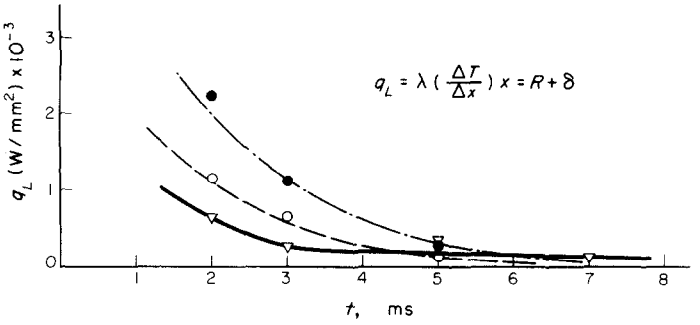

FIG. 11. Heat flux into surrounding liquid from superheated layer during bubble growth.

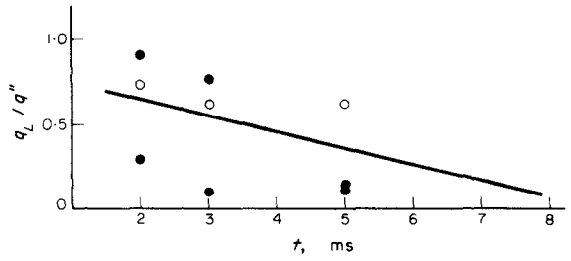

FIG. 12. Ratio q_L/q'' vs time.

4. CONCLUSION

The experimental and theoretical analysis of the temperature fields in the bubble and its liquid environment in pool boiling is considered. The analysis is performed for the case of a single growing bubble on a heated surface. The values which were found for the bubble radius from the filming of the bubble during bubble growth are in good agreement with the derived values which were obtained from analyzing the temperature field in the superheated liquid layer around the bubble. This is quantitative proof of the fact that

the bubble growth is controlled by the change in the temperature field around the bubble (e.g. heat transferred to the interface) in the time interval where liquid inertia and surface tension are not significant. A temperature field analysis subject to the conditions of this experiment for the region near the heating surface was not possible due to the physical limitations of the thermocouple which was used.

REFERENCES

1. N. Zuber, The dynamics of vapor bubbles in non-uniform temperature fields, *Int. J. Heat Mass Transfer* **2**, 83 (1961).
2. J. D. Van Stralen, The mechanism of nucleate boiling in pure liquids and in binary mixture, Parts I and II, *Int. J. Heat Mass Transfer* **9**, 995 (1966).
3. B. Mikic and W. Rohsenow, Bubble growth rates in non-uniform temperature field, in *Progress in Heat and Mass Transfer* Vol. II, p. 283 (1969).
4. C. Y. Han and P. Griffith, The mechanism of heat transfer in nucleate pool boiling, Parts I and II, *Int. J. Heat Mass Transfer* **8**, 887 (1965).
5. D. A. Labuntsov, Bubble growth mechanism on a heating surface, *Inzh. Fiz. Zh.* **6**, 4 (1963).
6. N. Afgan, An analysis of temperature fluctuation in pool boiling, *Zh. Prikl. Mekh. I Tekn. Fiz.* **5**, 5 (1973).
7. V. Pislar, N. Afgan, M. Stefanovic and Lj. Jovanovic, Determination of microthermocouple dynamics characteristics, *Int. Seminar on Heat and Mass Transfer*, Herceg-Novi, Yugoslavia (1969).
8. E. N. Ganic, Nucleate boiling bubble growth and departure, M.S. Thesis, University of Belgrade (1972).
9. V. I. Subbotin, D. N. Sorokin and A. A. Tsiganok, Some problems on pool boiling heat transfer, Paper B 1.9, in *Proceedings, Fourth International Heat Transfer Conference*, Paris–Versailles, Vol. V (1970).
10. J. M. Delay, J. P. Galoup, M. Reocreux and R. Ricque, Metrology of two phase flow: Different methods (Commissariat a l'Energie Atomique, Grenoble, France), Report CEA-R-4457 (1973).

ANALYSE DU CHAMP DE TEMPERATURE DANS UNE BULLE ET SON ENVIRONNEMENT D'EAU LIQUIDE EN EBULLITION

Résumé—On présente une étude expérimentale du champ de température dans une bulle et son environnement liquide. On considère aussi la vitesse de croissance de la bulle. Un modèle mathématique à une seule dimension du champ de température autour de la bulle est comparé aux résultats expérimentaux.

UNTERSUCHUNG VON TEMPERATURFELDERN IN BLASEN UND DER DIESE UMGEBENDEN FLÜSSIGKEIT BEIM BEHÄLTERSIEDEN VON WASSER

Zusammenfassung—Es wird über eine experimentelle Untersuchung der Temperaturfelder in Blasen und der diese umgebenden Flüssigkeit unter Berücksichtigung des Blasenwachstums berichtet. Für das Temperaturfeld in der Umgebung der Blase wird ein lineares mathematisches Modell entwickelt, das mit experimentellen Ergebnissen verglichen wird.

АНАЛИЗ ТЕМПЕРАТУРНЫХ ПОЛЕЙ ВНУТРИ ПУЗЫРЬКА И В ОКРУЖАЮЩЕЙ ЕГО ЖИДКОСТИ ПРИ КИПЕНИИ ВОДЫ В БОЛЬШОМ ОБЪЕМЕ

Аннотация — В работе представлен экспериментальный анализ температурных полей внутри пузырька и в окружающей его жидкости. Одновременно расматривается скорость роста пузырька. Разработанная одномерная математическая модель температурного поля вокруг пузырька сравнивается с экспериментальными данными.